



Research article

Curcuminoid (CRE-Ter)/Liposome as delivery platform for anti-osteoclastogenesis via NF- κ B/ERK pathways in RANKL-induced RAW 264.7 cells through PLA foamsYutthana Pengjam^{a,*}, Pharkphoom Panichayupakaranant^{b,c}, Varaporn Tanrattanakul^d^a Faculty of Medical Technology, Prince of Songkla University, Songkhla 90110, Thailand^b Department of Pharmacognosy and Pharmaceutical Botany, Faculty of Pharmaceutical Sciences, Prince of Songkla University, Hat-Yai 90112, Thailand^c Phytomedicine and Pharmaceutical Biotechnology Excellence Center, Faculty of Pharmaceutical Sciences, Prince of Songkla University, Hat-Yai 90112, Thailand^d Department of Materials Science and Technology, Faculty of Science, Prince of Songkla University, Songkhla 90110, Thailand

ARTICLE INFO

Keywords:

Curcuminoid (CRE-Ter)
Liposome encapsulates
NF- κ B/ERK pathways
Osteoclastogenesis
PLA foams

ABSTRACT

Aims: Curcuminoid (CRE-Ter) is the active component of turmeric, and is widely understood to offer anticancer, antioxidant, and anti-inflammatory properties. The drawbacks, however, include rapid metabolism and systemic elimination as well as minimal bioavailability. In an attempt to address the issue of bioavailability, this study seeks to encapsulate CRE-Ter in a liposome before its incorporation on PLA foams in order to inhibit the process of osteoclastogenesis which takes place in RANKL-induced RAW 264.7 cells.**Main methods:** Having encapsulated the CRE-Ter into the liposomes, the influence of the release of liposomal CRE-Ter from PLA foams in order to inhibit the process of osteoclastogenesis in the case of RANKL-induced RAW 264.7 cells was investigated. By measuring the decline in tartrate-resistant acid phosphatase (TRAP) content it was possible to evaluate the influence of CRE-Ter/Liposome upon osteoclastogenesis *in vitro*. Immunocytochemistry was employed to assess the marker for the monocyte/macrophage cells F4/80 content, while Western blots were used to evaluate the underlying mechanisms involved.**Key findings:** The findings demonstrate a novel method which employs tissue engineering scaffolds, which are produced to work alongside advanced additive manufacturing techniques with their basis in concepts from the field of alternative medicine. Initially, it was confirmed that CRE-Ter/Liposome at 20 μ g/ml is able to inhibit the creation of multinucleated osteoclasts which are induced by the receptor activator of the nuclear factor- κ B ligand (RANKL) in RAW 264.7 cells. It was shown that the CRE-Ter/liposome was able to increase the F4/80 content (F4/80 immunohistochemistry) in the RANKL treated RAW 264.7 cells. The TRAP content was lowered by the CRE-Ter/liposome along with the osteoclast-specific gene content such as cathepsin K, via the use of liposome-encapsulated PLA foams. When treated with CRE-Ter/liposome, RANKL-induced NF- κ B and ERK components such as NF- κ B-p65, ERK, phospho-NF- κ B-p65, and phospho-ERK pathways were all suppressed.**Significance:** The successful encapsulation of CRE-Ter into the liposomes offered a new opportunity to provide a new inhibitor of osteoclastogenesis and offers the possibility of developing treatments capable of addressing diseases which concern abnormal bone lysis.

1. Introduction

Available from the rhizomes found in turmeric (*Curcuma longa*), curcuminoids are compounds offering both hydrophobic and polyphenolic attributes [1]. The active constituents of curcuminoids include curcumin (Cu), bis-demethoxycurcumin (Bis), and demethoxycurcumin (De), but these have not yet been granted approval for medicinal

purposes due to their poor solubility when exposed to aqueous conditions, such as those found in the human gastrointestinal tract [2]. They are also unsuitable in the context of the liver and intestines where rapid metabolism occurs [3]. Consumption of curcuminoids across Southeast Asia is usually in the form of spices, while Indian Ayurvedic medicine has also long made use of curcuminoids. It is now known that curcuminoids have the potential to offer relief from diabetes, arthritis, multiple

* Corresponding author.

E-mail address: yutthana.p@psu.ac.th (Y. Pengjam).<https://doi.org/10.1016/j.heliyon.2021.e07823>

Received 3 August 2021; Received in revised form 10 August 2021; Accepted 16 August 2021

2405-8440/© 2021 The Author(s). Published by Elsevier Ltd. This is an open access article under the CC BY-NC-ND license (<http://creativecommons.org/licenses/by-nc-nd/4.0/>).

sclerosis, inflammation, indigestion, and colds [4, 5, 6, 7]. Under both *in vitro* and *in vivo* conditions, curcuminoids have also shown effectiveness against cancers, notably breast, ovarian, and lung cancer, as well as lymphoma, leukemia, and melanoma [8, 9, 10].

The balance of bone mass can be controlled through the homeostasis of osteoblasts which help to form bone, and osteoclasts which help in bone resorption. To ensure a balance in the bone mass, the relationship between the formation and resorption is critical and depends on the balance of these osteo-homeostasis functions. When a pathophysiological imbalance arises between the osteoclasts and osteoblasts, the outcome can be osteoporosis, which is a condition where the bone mineral density is very low, and fractures become commonplace as a consequence of the weakened bone structure. Cytokines along with hormones and growth factors play an important role in moderating the differentiation and activities of osteoclasts, which in turn support the signaling networks and particular transcription factors which contribute to the induction of target genes [11]. Multinucleated giant cell osteoclasts result from hematopoietic progenitors of monocyte/macrophage lineage cells such as the RAW 264.7 cells [12], via a process of differentiation which is primarily controlled through the receptor activator of the nuclear factor- κ B ligand (RANKL) which serves to interact with NF- κ B [13]. Osteoclastogenesis can be characterized as it accumulates phenotypic osteoclast markers. These signals include the expression of cathepsin K, TRAP (tartrate-resistant acid phosphatase) and also the physical change to form large multinucleated cells [14]. In the present, there are many nutraceutical compounds that are obtained from natural products and may offer the potential to serve as treatments for diseases of the bones which arise as a consequence of osteoclast-mediated excessive bone resorption [15, 16]. Turmeric or *Curcuma longa* L. has many pharmacological properties, including anti-osteoclastogenesis and suppressing NF- κ B [17].

Scaffold is used for supporting three-dimensional tissue formation and for performing some functions, such as supporting cell-cell scaffold interaction. Scaffold is obtained from artificial solid biomaterial. Scaffold is providing transport of nutrients, gases and metabolic waste for allowing cell bioactivities and mechanically supporting defective tissue, which prevents deformation of the growing tissue during tissue regeneration [18]. It has been shown that tissue engineering scaffolds have a useful role in repairing defects or a critical size following surgery through offering superior physical support as well as by enhancing the biocompatibility of the conditions in which *in vivo* tissue formation takes place [19]. Tissue engineering scaffolds printed in 3D form (3DP) can be ideal as a bone graft substitute due to their capacity to manage connectivity, pore geometry, and chemistry. Those pores which are connected can play a role in the transportation of nutrients, the removal of waste products, vascularization, and the ongoing ingrowth of new bone [20]. Scaffold is made from poly lactic acid (PLA) to form PLA foam using various preparation techniques, for example 3D printing, solid freeform fabrication, solvent casting including particle leaching, the thermal induction of phase separation, batch foaming which uses supercritical carbon dioxide, or sometimes a mixture of particle leaching along with batch foaming using supercritical carbon dioxide [21].

Although the therapeutic benefits of curcuminoids are clearly apparent, the curcumin molecule is not readily soluble in water, and its bioavailability is therefore restricted [22]. Intestinal and hepatic metabolism is rapid, and as a consequence this leads to up to 70% elimination via the bowel [23]. However, the curcuminoid-rich extract, CRE-Ter (CRE), which is highly soluble in water was initially dispersed in polyvinylpyrrolidone K30 (PVP K30) before being incorporated with hydroxypropyl- β -cyclodextrin (HPBCD). This offers the advantage that CRE-Ter is far more soluble than any of its principal active compounds [24, 25]. Moreover, a number of drug carriers have undergone development specifically to enhance curcumin bioavailability, with liposomes having been widely studied and now playing a prominent role [26, 27]. Liposomes are non-toxic spherical vesicles which are both biocompatible and biodegradable, and can effectively deliver drugs. They can improve

both tissue and cellular drug uptake, as well as supporting the distribution of specific compounds to the sites which are the targets for the therapy [28]. Phospholipid nanovesicles are able to encapsulate two different drug types: hydrophobic and hydrophilic. Hydrophobic drugs, also known as lipophilic drugs, can be trapped using the bilayer membrane, while in contrast, the location of hydrophilic drugs will be within the aqueous center [29]. This research demonstrates the effective liposome encapsulation of the curcuminoid biomolecule (CRE-Ter) and its hydrophobic properties, and further goes on to incorporate the liposome in PLA foams. The role of the foam is to offer physical support during cell attachment, allowing a prolonged release of the drug from the liposome, which leads to enhanced bioavailability and reduced toxicity. The overall therapeutic index is therefore raised by this approach. Through the course of this research, the authors are now considering the integration of 3DP technology with effective alternative medicine use, since this may offer superior outcomes in tissue engineering. It has been clearly revealed by the findings that the CRE-Ter-encapsulated liposomes within a tissue engineering scaffold were able to restrict the process of osteoclastogenesis. No signs of cytotoxicity were observed to affect the healthy RANKL-induced RAW 264.7 cells or the osteoclast cells, thereby supporting filopodial prosthesis adhesion, proliferation, and formation upon the surface of the PLA foam.

2. Materials and methods

2.1. Reagents

TRAP activity was examined through the use of a leukocyte acid phosphatase assay kit supplied by Sigma (St. Louis, MO, USA). Qiagen (Valencia, CA, USA) supplied the RNease kit for RNA extraction, while RANKL was obtained from R&D System (Minneapolis, USA). Gibco Co. (Bangkok, Thailand) supplied RPMI 1640 with 10% heat inactivated FBS, 100X antibiotic-antimycotic, and 2 mM glutamine. The remaining reagents employed during this research were obtained from Sigma Chemical Co. or Wako Pure Chemical Industries Ltd. (Bangkok, Thailand). The extract CRE-Ter, comprising 14% w/w curcuminoids, underwent preparation and standardization through the technique explained previously [24, 25]. NatureWorks LLC (Blair, NE, USA) supplied the PLA (4042D grade), while Sigma-Aldrich Co., Ltd. (Bangkok, Thailand) supplied the sodium hydroxide and 3-glycidyloxypropyl trimethoxysilane (GPMS). Natural RWS, comprising cellulose (39%), hemicellulose (29%), lignin (28%), and ash (4%) was provided by Khoa Mahachai Parawood Co., Ltd. (Thailand). Two different ranges for the particle sizes of RWS were employed: 212–600 μ m and \leq 75 μ m. The smaller range (\leq 75 μ m) was produced through a process involving the grinding of large particles (212–600 μ m) in liquid nitrogen with a NanoTech NT-500D grinder operating at 25,000 rpm, whereupon a sieve was used to process the final product. GREATCHEM and Supply Pty., Ltd. (Shandong, China) supplied the azodicarbonamide (AZDC) while Kit Phaibun Chemistry Ltd. (Bangkok, Thailand) provided the zinc oxide. The silane coupling agent used was GPMS, while AZDC served as a blowing agent and ZnO was employed as the accelerator in the foaming procedure. Sigma Aldrich provided the OS medium, which comprised 10 mM β -glycerophosphate, 50 mg/mL ascorbic acid, and 100 nM dexamethasone.

2.2. Preparation of CRE-Ter

CRE-Ter (with curcuminoid content of 14% w/w) was produced via the approach described earlier [24, 25]. Initially, methanol was used to extract the dried turmeric powder through microwave-assisted extraction with a power setting of 900 Watt, and a temperature in the range of 70–75 $^{\circ}$ C, using three irradiation cycles, whereby one cycle involved operation with power on for three min and 30 s for power off. The resulting extract was then filtered before eluting using a Diaion[®] HP-20 column with 55% and 60% v/v ethanol in order to produce the

curcuminoid-rich extract (CRE). Solvent evaporation was the method employed to prepare the CRE-Ter. In the initial step, CRE was dispersed through polyvinylpyrrolidone K30 (PVP K30) (9% w/w), before incorporation with hydroxypropyl- β -cyclodextrin (HPBCD) in a molar ratio of 1:1. Solvent evaporation followed under reduced pressure in order to produce the CRE-Ter powder. According to the results of the HPLC analysis, the curcuminoid content of CRE-SD was around 14% w/w (Figure 1).

2.3. PLA biocomposite foam preparation

Extrusion was used to prepare the PLA compounds, whereupon compression molding was employed to produce the necessary PLA biocomposite foams. PLA and RWS with a weight ratio of 95:5 underwent melt-blending using a corotating screw extruder (PRISM TSE16TC) which had a 15:1 L:D ratio. Since the screws were short, it was necessary to extrude the materials twice in order to achieve a blend which was homogeneous. The initial extrusion was performed at varying temperatures of 140 °C and 165 °C in three different zones: feed, middle, and die. A screw speed of 100 rpm was maintained. In this current research, the foam production via AZDC decomposition can be performed solely inside the compression molding machine, and not in the extruder. Accordingly, pelletizing the extrudate and then extruding once again while including AZDC and ZnO in the blend, was carried out using a reduced temperature profile (130 °C, 150 °C, and 150 °C respectively at the feed, middle, and die points) in order to ensure that AZDC did not decompose inside the extruder. PLA degradation could be held to a minimum through the use of a greater screw speed or around 150 rpm which served to shorten the time spent in the extruder. Meanwhile, the respective AZDC and ZnO content levels were 1.94 and 0.06 wt %. Samples of the biocomposites which had been prepared were placed in a closed mold of size 130 × 130 × 2 mm and compression molded for 10 min at a temperature of 145 °C and pressure of 150 kg cm⁻².

2.4. Liposome size, zeta potential, and polydispersity index

An approach involving dynamic light scattering via Zetasizer Nano-S equipment (Malvern Instruments, Malvern, UK) was employed to measure the size of the liposomes and the polydispersity index (PDI). Sizes were given in terms of the mean liposomal hydrodynamic diameter (nm). Where the PDI values did not exceed 0.5, this was indicative of a monodisperse and homogeneous population. The vesicle surface charge could be established via correlation spectroscopy using measurements of

electrophoretic mobility (μ), which was accomplished with the Zetasizer Nano-S equipment. The findings were stated in terms of zeta potential (Z , mV) following the use of the Smoluchowski equation to convert μ to Z : in this case, $Z = \mu\eta/\epsilon$, in which η represents viscosity, and ϵ indicates the solution permittivity. These measurements were taken at room temperature, while 200 μ L of samples underwent dilution using a citric-phosphate buffer solution (1/20).

2.5. CRE-Ter loaded liposomes

The approach set out below was used to prepare the liposomes. A suitable POPC aliquot (1-palmitoyl-2-oleoyl-phosphatidylcholine, supplied by Avanti Polar Lipids, Alabama, United States), was dissolved using chloroform and placed in a round-bottom flask before drying at low pressure using a rotary evaporator at a temperature of 40 °C. The outcome was the formation of a thin lipid film inside the flask upon the inner wall. The resulting phospholipid film was stored overnight at a temperature of 4 °C prior to being rehydrated using PBS buffer (pH 7.4). This was followed by 30 min of sonication. A UV lamp was used for 2 h to sterilize the liposomes, whereupon a suitable quantity of CRE-Ter in DMSO was introduced to the liposomal suspension until the resulting molar ratio of POPC to CRE-Ter was 25:1 [30, 31, 32].

2.6. CRE-Ter loading efficiency in POPC liposomes

Liposome preparation was carried out as explained previously [30, 31, 32]. To determine the embedded CRE-Ter percentage by extracting the CRE-Ter which was entrapped from the liposomes, the liposomal suspension was filtered using a Sephadex G-25 column. The Sephadex column underwent elution with milliQ water, whereupon the entrapped CRE-Ter was measured via UV-Vis spectrophotometry ($\epsilon_{434\text{nm}} = 10,997$).

2.7. In vitro release of liposome-encapsulated CRE-Ter

The *in vitro* study of CRE-Ter release required the use of dialysis tubings (MW cutoff 12,000–14,000 Da) which were supplied by Carolina Biological Supply Company (NC, USA). These were immersed overnight in DI water to eliminate the presence of preservatives. A pair of dialysis sacs were then prepared: the first had free CRE-Ter serving as the control, while the second contained liposomal CRE-Ter. The phosphate buffered saline (PBS) at a pH of 7.4 was prepared using 25% v/v of methanol. After the sacs had been sealed, a glass rod was used to place them fully

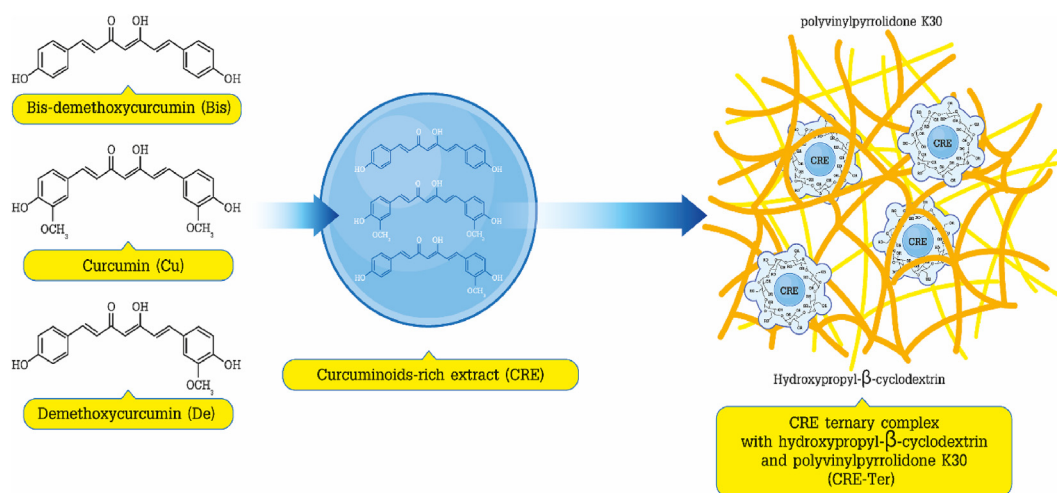


Figure 1. CRE-Ter chemical structure. CRE-Ter was prepared using dried turmeric powder to obtain CRE (curcuminoids enriched extract). CRE was initially dispersed using polyvinylpyrrolidone K30 (PVP K30), before being incorporated in hydroxypropyl- β -cyclodextrin (HPBCD). Following HPLC analysis, it was determined that the curcuminoid content of CRE-Ter was 14% w/w.

into a flask containing the buffer solution. This flask was then maintained at 37 °C while stirring constantly with a magnetic stirrer at 150 rpm. At specified intervals, samples were collected and absorbance measurements were obtained with a BioTek Synergy 2 SLFPTAD microplate reader (BioTek, Winooski, VT, USA).

2.8. Cell culture and CRE-Ter loaded liposome seeding

The RAW 264.7 cells underwent culturing in RPMI 1640 medium with added 10% heat inactivated FBS, 100 U/ml penicillin G, 2 mM glutamine, and 100 µg/ml streptomycin sulfate, under humid conditions in a 5% carbon dioxide atmosphere at a temperature of 37 °C. Having reached the stage of semi-confluence, the cells were collected using 0.25% trypsin (Sigma) and 0.02% ethylene diaminetetraacetic acid, prior to seeding on the PLA foam scaffolds. Before seeding with cells, sterile PLA foams were washed twice with sterilized water for 5 min each, and then rinsed in phosphate-buffer saline (PBS) solution three times before immersion for 10 min in RPMI 1640 medium for 10 min. The PLA foams were then put into culture plates (6-well, 12-well, or 24-well) and seeded with 5×10^3 cells, in order to produce the RAW cell-PLA foams. These RAW cell-PLA foams underwent treatment using 20 ng/ml RANKL along with varying liposomal CRE-Ter doses for a range of different time intervals, and were monitored for cell adhesion, proliferation, migration, and expression of osteoclast markers. The culture medium was replenished every 3 days. PLA foams without cells and cell-PLA foams without liposomal CRE-Ter were used as controls.

2.9. Cell cytotoxicity and viability assays

The RAW cell-PLA foams which had been treated for a 5-day period RANKL (20 ng/ml), in the presence and absence of various liposomal CRE-Ter doses (1, 2.5, 5, 10, 20, or 30 µg/ml) underwent further cell viability analysis via MTT assay. The assay relies upon the fact that there will be a reduction in yellow tetrazolium MTT to form an insoluble formazan salt as a consequence of the effects of the metabolically active cells on the PLA foams. A spectrophotometer is then used to measure the intracellular purple formazan following solubilization. After a 5-day treatment period, the cell-PLA foams underwent further treatment for 4 h using MTT at a temperature of 37 °C. The formazan crystals acquired were then dissolved with dimethylsulfoxide whereupon absorbance measurement was performed using 100 µl of the conditioned medium at 540 nm (Thermo scientific, Multiskan FC, Pittsburgh PK, United States).

2.10. TRAP assay for osteoclastogenesis confirmation

The RAW cell-PLA foams underwent treatment with 20 ng/ml RANKL for a range of different time periods of 1, 2, 3, 4, and 5 days in a chamber under humid conditions with a 5% carbon dioxide atmosphere at a temperature of 37 °C. At the conclusion of each time interval, the TRAP assay was carried out using the kit provided by TaKaRa Bio., Inc. (Tokyo, Japan) in line with the guidance of the manufacturer. The results are presented in the form of TRAP activity against days.

2.11. Real-time PCR for osteoclastogenesis confirmation

The RAW cell-PLA foams underwent treatment both in the presence and absence of RANKL (20 ng/ml) along with liposomal CRE-Ter (10 or 20 µg/ml) prior to incubation for a range of time intervals of 1, 2, 3, 4, and 5 days in a chamber under humid conditions with a 5% carbon dioxide atmosphere at a temperature of 37 °C. An RNeasy mini kit (Qiagen, USA) was used to isolate total RNA, while the synthesis of cDNA was carried out with the ReverTra Ace qPCR kit (Toyobo, Osaka, Japan) in line with the guidance of the manufacturer. The real-time PCR of the osteoclast marker genes was carried out using the Fast-Start SYBR Green Master mix (Roche Diagnostic, Mannheim, Germany) with particular primers as listed below, using a Gene Atlas thermocycler (Astec Co, Japan).

Cathepsin K Forward: 5' – ATGTGGGGGCTCAAGGTTCTG – 3'
Reverse: 5' – CATATGGGAAAGCATCTTCAGAGTC – 3'
GAPDH Forward: 5' – AAATGGTGAAGGTCCGGTGTG – 3'
Reverse: 5' – GAATTTGCCGTGAGTGGAGT – 3'

Image Quant TL (GE healthcare Life Sciences) along with an LAS4000 chemiluminescence detector (Fujifilm, Japan) was used to calculate the relative expression levels of the target genes in this study to compare with glyceraldehyde 3 phosphate dehydrogenase (GAPDH) used as the endogenous reference.

2.12. Osteoclastogenesis inhibition confirmation by acid phosphatase staining

The RAW cell-PLA foams underwent treatment with 20 ng/ml RANKL, in the presence or absence of 20 µg/ml CRE-Ter in a chamber under humid conditions for a 5-day period in an atmosphere of 5% carbon dioxide at 37 °C. The cells were then stained using acid phosphatase and examined using a light microscope. Where purple/dark red granules could be observed, these were indicative of acid phosphatase positive cells.

2.13. Immunocytochemistry for anti-mouse F4/80

The RAW cell-PLA foams underwent treatment with CRE-Ter (20 µg/ml) prior to incubation for a 5-day period both in the presence and absence of RANKL (20 ng/ml). Following incubation, the cell-PLA foams were rinsed in PBS before fixing for 10 min in 4% Paraformaldehyde (PFA) with Phosphate-Buffered Saline (PBS). To block the cellular endogenous peroxidase activity, 0.3% hydrogen peroxide in absolute methanol was used for a period of 15 min. Pre-incubation of the cell-PLA foams was carried out using 500 µg/ml normal goat IgG dissolved in 1% BSA in PBS for 1 h at a pH value of 7.4. The reactions were all performed at room temperature except when stated otherwise. The cell-PLA foams underwent incubation for a 2-hour period with anti-mouse F4/80, whereupon they were washed with 0.075% Brij 35 in PBS and further incubated for 1 h in the presence of HRP-conjugated goat anti-rat IgG in 1% BSA in PBS. Having washed the cell-PLA foams with 0.075% Brij 35 in PBS, the foams then underwent incubation in darkness with DAB and hydrogen peroxide with nickel and cobalt ions also present. The slides were then mounted in order to capture the necessary images using an Olympus microscope attached to a digital camera to provide $\times 100$ magnification.

2.14. Western blot analysis

The RAW cell-PLA foams underwent treatment with 20 ng/ml RANKL along with a variety of different liposomal CRE-Ter (10 or 20 µg/ml) dosages for a 5-day period. NE-PER reagent (Thermo-Scientific Inc., Washington DC, USA) was used to obtain the cytoplasmic and nuclear proteins in line with the guidance of the manufacturer. SDS-PAGE gel was then used to separate the proteins which were subsequently transferred to a polyvinyl difluoride (PVDF) membrane. This PVDF membrane was then washed prior to incubation with a number of specific antibodies (anti NF-κB-p56, anti-phospho NF-κB-p65, anti ERK, anti-phospho ERK, and anti β-actin, provided by Cell Signaling, Beverly, MA, USA). Following a second wash, the membrane was then treated for 1 h using a secondary antibody in conjugation with horseradish peroxidase. The Chemiluminescence Vilbers (Fusion Solo S) digital imaging system (Vilber, France) was then used to detect the protein bands.

2.15. Statistical analysis

The data are presented in the form of mean \pm SD. The statistical tests carried out included one-way ANOVA with a post hoc Dunnett's test or Student's t-test. The significance levels for these tests were set to $P < 0.05$.

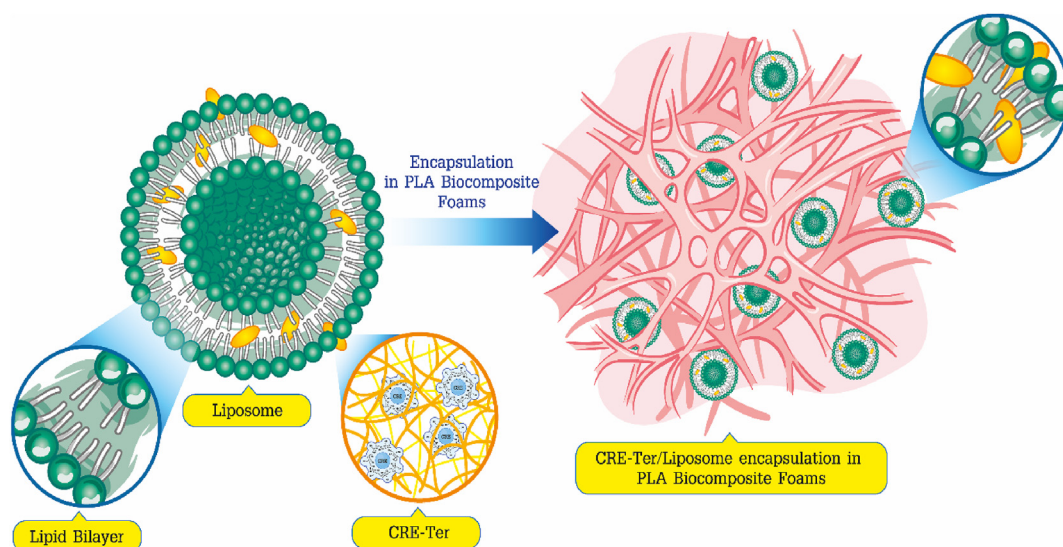
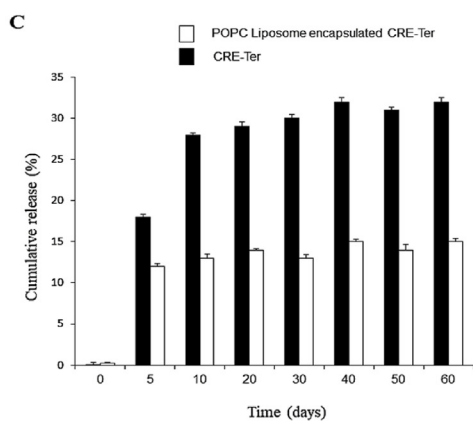
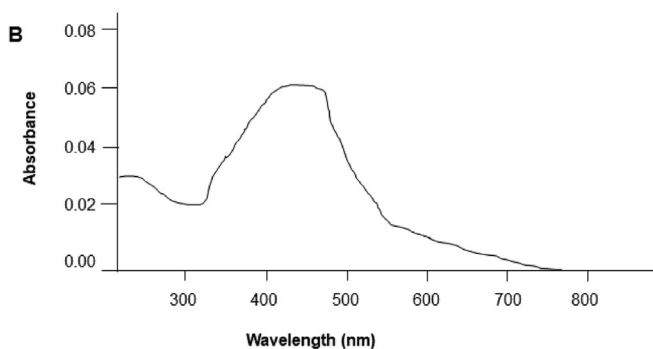


Figure 2. The 3D PLA foam chemical structure along with that of liposome-encapsulated CRE-Ter is presented. The liposomes underwent 2 h of sterilization using a UV lamp, whereupon a suitable quantity of CRE-Ter in DMSO was introduced to the liposomal suspension to achieve a molar ratio for POPC to CRE-Ter of 25:1.

A

Systems	Dimension/nm	Polydispersity	Z-potential/mV
POPC liposomes	330.0 ± 15.2	0.42 ± 0.01	- 24.38 ± 0.81
CRE-Ter POPC liposomes	386.6 ± 26.2	0.42 ± 0.01	- 30.55 ± 1.62

Figure 3. (A) The size, polydispersity, and zeta potential for the liposomes in the study. (B) The UV-Vis spectrum for the elution of the Sephadex G25 column with milliQ water. (C) The *in vitro* release of liposome-encapsulated CRE-Ter, where CRE-Ter from liposomes demonstrates controlled release at 15% after a 60-day period, while the release of free curcumin reached 31.3%. (D) MTT assay measurements of seeding efficiency for PLA foams and PLA foams with liposome at 12 h after seeding (n = 3).



D

Samples	Seeding efficiency (%)
PLA foams	55.22 ± 1.45
PLA foams with POPC Liposome	63.55 ± 1.99

3. Results

3.1. Curcuminoid (CRE-Ter) encapsulation with liposome

To investigate the functional significance of liposomal CRE-Ter-loaded PLA foams for tissue engineering, we encapsulated CRE-Ter into liposomes (Figure 2) as per standard procedure [34, 35]. The CRE-Ter enriched liposomes had marginally increased dimensions, as a clear consequence of the solubilization of the CRE-Ter and DMSO in the POPC bilayer. The preparation of liposomes via sonication resulted in poly-disperse samples as expected. There was a decline in zeta potential as a result of the change from pure POPC liposomes to CRE-Ter-enriched liposomes, as shown in Figure 3A. This can be attributed to the partial deprotonation of phenolic moieties ($pK_a = 8.14 \pm 0.40$; calculations were carried out with the support of Advanced Chemistry Development (ACD/Labs, Software V11.02)) as well as the use of buffered pH and the associated outcome of dissociation of the phenoxide groups which were exposed to the aqueous bulk. When arranged in this manner, applying the latest organic solvent-free, pH-driven liposomal encapsulation of CRE-Ter in liposomes, the effects were particularly notable since we added the CRE-Ter to preformed liposomes to avoid the problem of CRE-Ter photodegradation. Furthermore, UV irradiation was employed to sterilize the liposomes before CRE-Ter was added. It was confirmed that the entrapment of CRE-Ter in the bilayer reached 95.2% as shown in Figure 3B. Furthermore, the influence of polyvinylpyrrolidone K30, which acts as a pore-forming agent and therefore may have an impact upon both the structure and performance of the PLA foams, was examined using a standard approach [36, 37]. Also investigated was the influence of hydroxypropyl- β -cyclodextrin (HPBCD), which also acts as a pore-forming agent, again using a standard approach [38]. In this research, it was determined that there was no effect upon the elasticity of the liposome exerted by the HPBCD complex in the PLA foam. The results thus far strengthen the concept that polyvinylpyrrolidone K30 and HPBCD did not interfere with the PLA scaffolds in this study (not shown).

3.2. In vitro liposome-encapsulated curcuminoid (CRE-Ter) release

In Figure 3C, the release profiles for *in vitro* CRE-Ter from liposomes are presented for the study period of 60 days. It can be seen that by the end of the time period, 15% of the CRE-Ter had been released in the case of liposome encapsulation, while for free CRE-Ter, the release amounted to 31.3%. It can be concluded that the release in the liposome-encapsulated context was performed in a more controlled and sustained manner over the 60-day period than is the case for the free CRE-Ter.

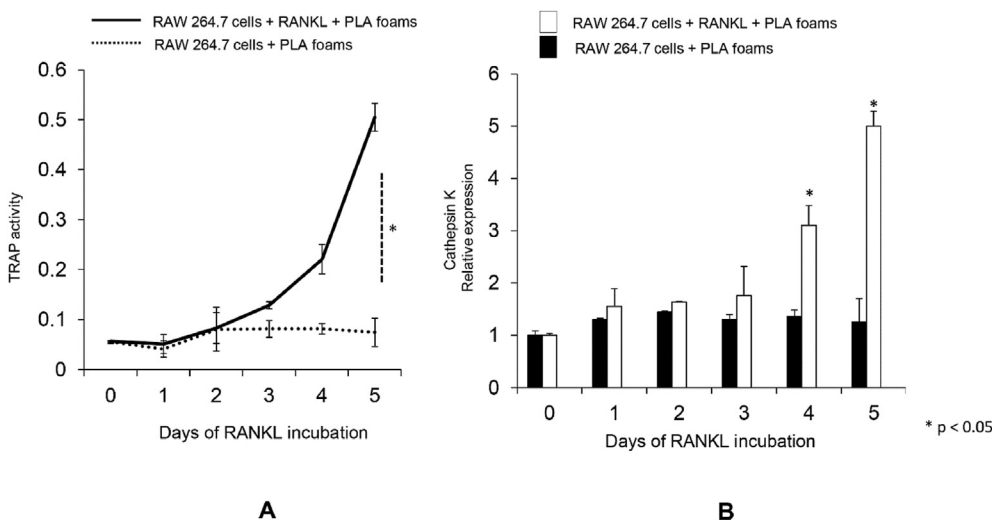


Figure 4. Osteoclastogenesis testing through PLA foams. (A) The RAW 264.7 cells underwent treatment in the presence or absence of RANKL (20 ng/ml) for differing time periods using PLA foams. Measurements were taken for the osteoclast marker protein TRAP at 0, 1, 2, 3, 4, and 5 days in each group following a standard procedure. The values are presented in terms of the activity of TRAP content in cells. (B) The real-time PCR assay for cathepsin K genes in the RAW 264.7 cells undergoing treatment in the presence of absence of RANKL (20 ng/ml) for different time periods (0, 1, 2, 3, 4, or 5 days). The internal control was GAPDH gene expression, while mRNA expression was shown as the relative expression between cathepsin K and GAPDH. The statistical significance level was set to $P < 0.05$ for comparisons between days.

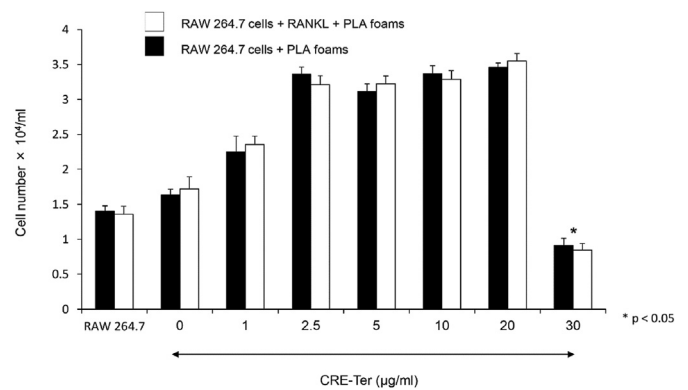


Figure 5. Cytotoxicity measurements for CRE-Ter using PLA foams were taken via MTT assay. The RAW 264.7 cells underwent treatment using different CRE-Ter concentrations (0, 1, 2.5, 5, 10, 20, and 30 µg/ml) for a 5-day period in the presence and absence of the osteoclast inducer RANKL (20 ng/ml) as described in the Materials and Methods section. The viable cells were then counted. The results are presented in the form of mean \pm SD for the six experiments performed independently. Statistical significance levels of comparisons between the CRE-Ter group and the control were determined at the level of $P < 0.05$.

3.3. Biological evaluation in vitro

Calculation of the seeding efficiency allowed evaluation of the liposome incorporation influence upon osteoclast cell attachment as shown in Figure 3D. Improved seeding efficiency was reported for liposome-loaded scaffolds as a consequence of the greater surface area in comparison to the PLA foams used as the control.

3.4. RANKL- induces the RAW 264.7 cells into osteoclasts via PLA foams

The differentiation of RAW 264.7 cells into osteoclasts can be recognized through the presence of mature phenotypic osteoclast markers, such as the expression of cathepsin K and TRAP (tartrate-resistant acid phosphatase), in addition to physical changes to form large multinucleated cells [39]. For the purpose of confirming this particular transition, a time course evaluation of RANKL activity was performed over a 5-day period using foams. The findings revealed that the RAW 264.7 cells which had been treated with RANKL (20 ng/ml) were able to differentiate into osteoclasts within 4 days using the PLA foams. This change was characterized by heightened TRAP activity and over-expression of cathepsin K mRNA (Figure 4A and B). This study confirms

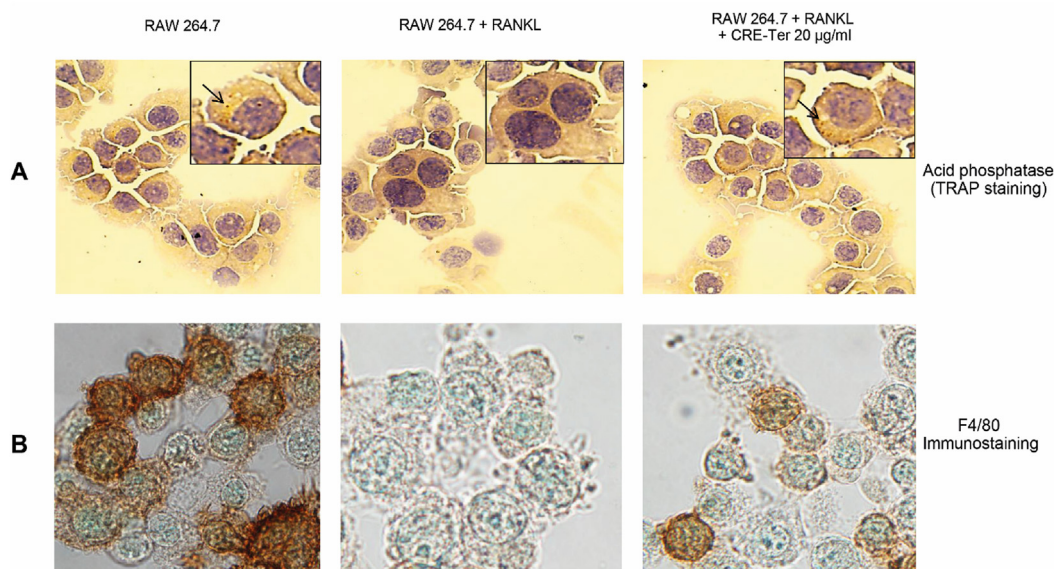


Figure 6. The differentiation of RAW 264.7 cells to osteoclasts using PLA foams. (A) Morphology of cells. (B) Semi-confluent RAW 264.7 cells underwent treatment using RANKL (20 ng/ml) and were subsequently co incubated for a 5-day period in CRE-Ter or without RANKL. The immuno-cytochemical studies examining the macrophage marker F4/80 were performed as explained in the Materials and Methods section, and cell photography was carried out using 100× bright field microscopy.

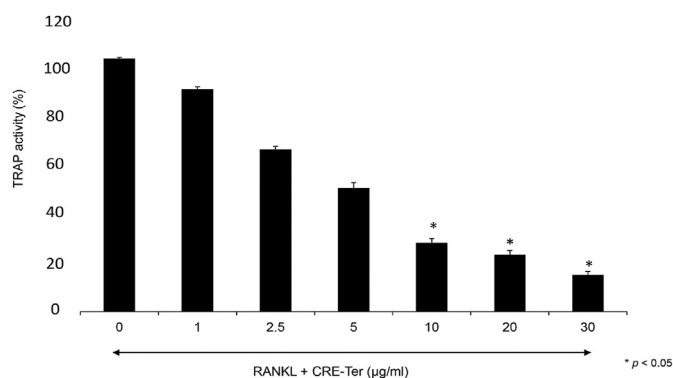


Figure 7. The differentiation of RAW 264.7 cells to osteoclasts measured via TRAP activity. The semi-confluent RAW 264.7 cells underwent treatment using RANKL (20 ng/ml) and were subsequently co-incubated for a 3-day period in CRE-Ter or without RANKL. A standardized process was followed for whole cell TRAP staining and all cell photography was performed using 100× bright field microscopy. Statistical significance levels of comparisons with the osteoclasts were determined at the level of $P < 0.05$.

earlier findings which show that RANKL (20 ng/ml) is able to induce the transition of undifferentiated RAW 264.7 cells into osteoclasts [16].

3.5. Cell viability and cell cytotoxicity assay through PLA foams

To measure the cell viability and cytotoxicity in the case of liposomal CRE-Ter, the RAW cells which had been seeded upon PLA foam scaffolds underwent treatment using a range of different CRE-Ter concentrations (0, 1, 2.5, 5, 10, 20, or 30 µg/ml) over a 5-day period both in the presence and absence of RANKL (20 ng/ml), and were then subjected to MTT assays. Liposomal CRE-Ter did not show any cytotoxic effects up to 20 µg/ml. However, longer exposure of the cells to 20 µg/ml liposomal CRE-Ter caused the number of viable cells to fall, which is clearly apparent from the MTT assay results shown in Figure 5. Therefore, further experiments were performed using CRE-Ter at concentrations up to 20 µg/ml.

3.6. CRE-Ter abrogates RAW 264.7 cells differentiation through PLA foams

The RAW cells which were grown using PLA foam scaffolds underwent treatment with RANKL both in the presence and absence of CRE-Ter for 5-day period under the conditions described earlier. Morphological and histochemical analysis assessed the differentiation of the RAW cells to form osteoclasts. The use of RANKL treatment helped to produce multi-nucleated cells which then stained positive for acid phosphatase, which appeared as purplish to dark red granules in cytoplasm (Figure 6A). Cells co-treated with 20 µg/ml liposomal CRE-Ter did not exhibit multi-nucleated morphology. They did not stain positive for acid phosphatase. When RAW 264.7 cells were treated using a combination of RANKL and 20 mg/ml liposomal CRE-Ter, the outcome was a decline in the specific RAW 264.7 macrophage markers when F4/80 staining was performed. In contrast, when cells were treated using 20 mg/ml liposomal CRE-Ter, the F4/80 staining was strong, demonstrating the cells' macrophage status as indicated in Figure 6B. Cells which had undergone co-treatment with liposomal CRE-Ter were able to exhibit inhibition of the differentiation of RAW 264.7 cells to osteoclasts on the basis of dosage, as well as lowering TRAP activity (Figure 7). These findings add further weight to the idea that liposomal CRE-Ter is able to prevent RAW 264.7 cell differentiation into osteoclasts in the case of cells grown on PLA foams.

3.7. CRE-Ter decreases NF-κB/ERK pathways signaling protein through PLA foams

The RANKL-induced differentiation of osteoclasts requires NFκB to be activated, followed by Cathepsin K expression [12, 16]. Western blot analysis revealed that liposomal CRE-Ter systematically and significantly inhibited NF-κB pathway components, both NF-κB-p65 and p-NF-κB-p65, ($p < 0.05$) (Figure 8A and B). It is understood that the ERK signaling pathway plays a role in the survival, proliferation, and apoptosis of osteoclasts, along with their formation, polarity, podosome disassembly, and differentiation. RANKL is an osteoclastogenesis factor which has a significant role in osteoclast differentiation due to its ability to induce ERK phosphorylation [40]. Western blot analysis also revealed that liposomal CRE-Ter systematically inhibited ERK pathway components,

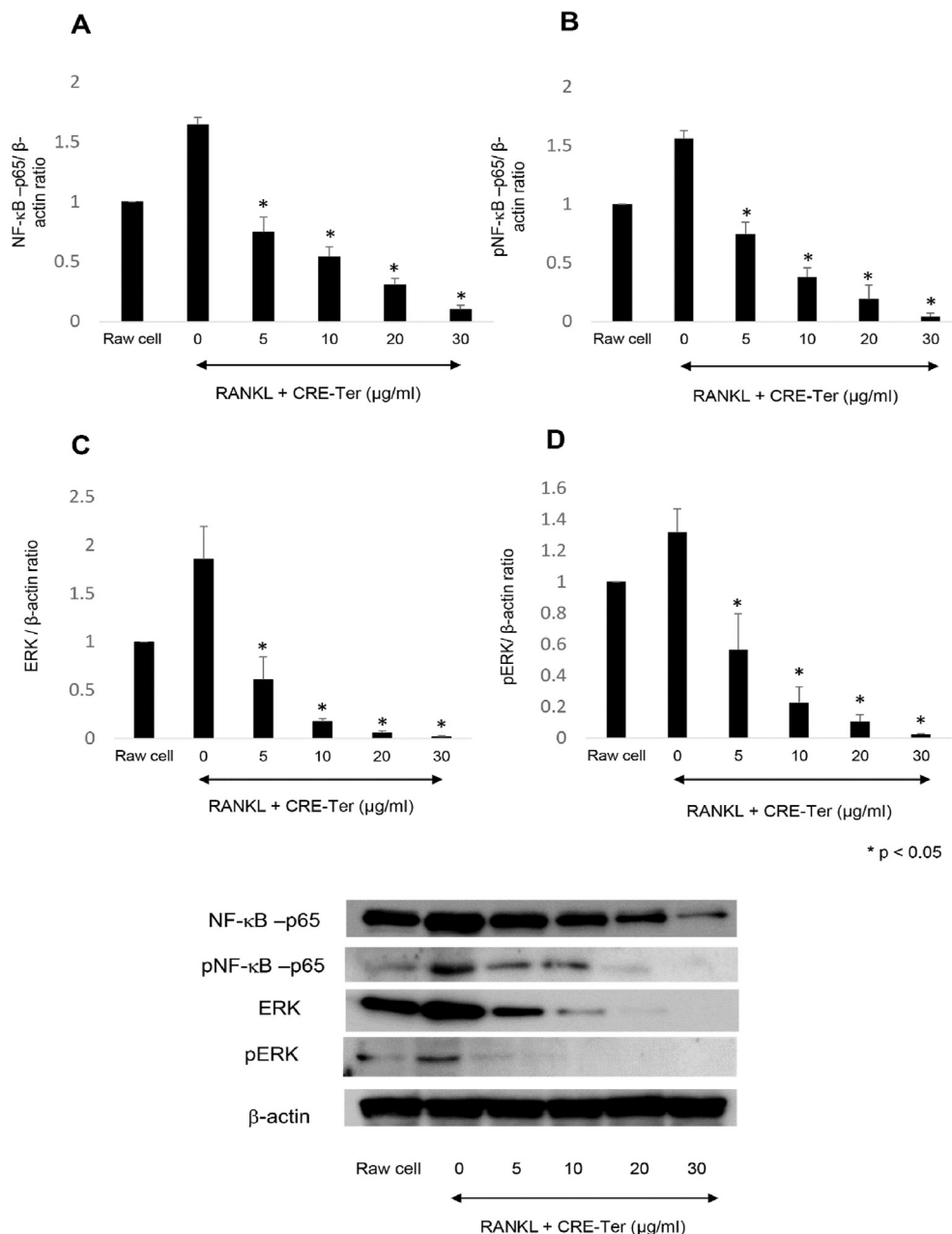


Figure 8. Influence of curcuminoid extracts upon the NF-κB and ERK pathways. Western blot analysis was carried out on NF-κB-p56, p-NF-κB-p65, ERK and p-ERK, with β-Actin serving as the internal control. Statistical significance levels of comparisons with the control were determined at the level of $P < 0.05$.

ERK and p-ERK, in a significant manner ($p < 0.05$) (Figure 8C and D). We believe that this inactivation leads to the repression of NF-κB and ERK signaling pathways, which are regulators of successive steps involved in osteoclast differentiation and activation. Cathepsin K are key regulators of osteoclast differentiation and bone remodeling, and are regarded as markers of mature osteoclasts [41]. The results of the real-time PCR and Western blot analyses revealed that liposomal CRE-SD was able to lower the gene expressions of cathepsin K in line with the dose given (Figure 9). This finding further supports the idea that the differentiation into osteoclasts of RAW 264.7 cells grown through PLA foams can be prevented by liposomal CRE-Ter.

4. Discussion

There is significant research interest in natural biomolecules such as curcuminoids because they are believed to offer the potential to deliver

therapeutic benefits via their inherent properties, while avoiding the problematic side effects which can result from the use of cytotoxic therapies [42]. Curcumin is understood to offer therapeutic qualities in limiting osteoclastogenesis through blocking the initiation and subsequent proliferation of osteoclasts. The antioxidant abilities of curcumin are based on the presence of hydroxyl groups within its chemical structure, while the antiproliferative and anti-inflammatory properties result from the presence of methoxy groups [43]. A number of novel delivery approaches have been considered in the recent past, among which are those systems which involve polymeric implantable delivery, capable of enhancing drug bioavailability. Bone turnover has also been treated using liposomal curcumin following a cell-based osteoarthritis model [44]. This research involved the optimization of the liposomal formulation via POPC (1-palmitoyl-2-oleoyl-phosphatidylcholine) in order to enhance the delivery systems through the liposomes used with curcuminoids. Previous studies have shown that POPC liposomes have the potential to enhance

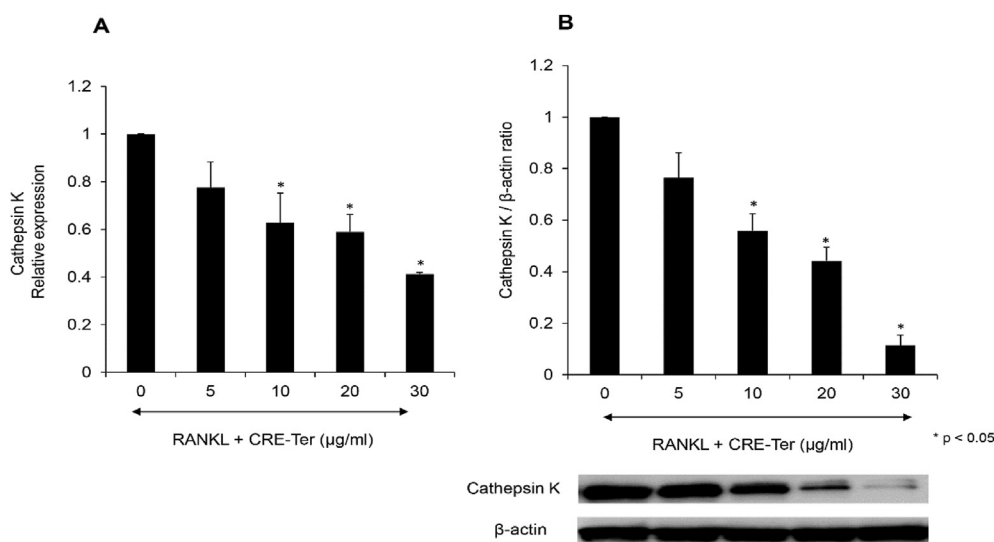


Figure 9. Effects of CRE-Ter on cathepsin K mRNA activity and cathepsin K protein. The RAW 264.7 cells underwent seeding in culture plates and treatment for a 3-day period using various CRE-Ter concentrations, or with RANKL (20 ng/ml), or with both. (A) Cathepsin K mRNA expression. (B) Cathepsin K protein expressed in terms of the mean ratio between cathepsin K, GAPDH, and β-actin. The GAPDH gene and β-actin protein expressions acted as internal controls. Statistical significance levels of comparisons with the control were determined at the level of $P < 0.05$.

curcumin bioavailability in rat model systems, while those liposomes which were composed with POPC offered improved efficiency of entrapment when compared to other lipids [35, 45].

In the study of bilayer stability, the stability of CRE-Ter in the lipid bilayer was examined along with the influence of the cationic agent. The study examined the size of vesicles, polydispersity index, and zeta potential. It was reported that those formulations which had a charge experienced a decline in the surface charge over time. Neutral formulations, however, saw the values for this parameter remain unchanged throughout the period of study. When lipid compounds were introduced to the bilayer, this resulted in the lipids undergoing an inner rearrangement, lowering the zeta potential. In the case of the CRE-Ter liposome, however, although the size increased, the polydispersity index did not. These findings showed that a stable lipid bilayer was produced. From a further study, the results of this current research showed high entrapment efficiencies of curcuminoid (CRE-Ter) (>90%) and significant stability over 50 days by using an *in vitro* liposome-encapsulated curcuminoid (CRE-Ter) release. Furthermore, improved seeding efficiency was demonstrated by liposome-loaded scaffolds.

Having managed to encapsulate the curcuminoid (CRE-Ter) successfully into the liposomes to achieve liposome-encapsulated CRE-Ter release, the authors investigated the effect of liposomal CRE-Ter on the RAW 264.7 cells and the osteoclast cells which had been cultured on PLA foams. It is widely understood that PLA foams are biodegradable, aliphatic thermoplastic polyesters which are commonplace as drug delivery agents, tissue engineering scaffolds, or implants. Artificial PLA foam is a porous biomaterial which can support the *in vivo* and *in vitro* processes of cell adhesion, proliferation, and differentiation, as well as the formation of tissue [46, 47]. PLA foam was reported to be non-toxic to MG-63 osteoblast-like cells [21]. The current data show that PLA foam did not exhibit cytotoxic effects on RAW 264.7 macrophages, and was safe for use in scaffold preparation for tissue engineering. Further study revealed that liposomal CRE-Ter dampened RANKL was able to initiate the process of osteoclast differentiation, which was measured through observation of TRAP activity, multinucleation, and the upregulation of the osteoclast-specific gene, cathepsin K. The findings suggest that when liposomal CRE-Ter is cultured on PLA foams, it will be capable of restricting osteoclast differentiation through the attenuation of the cellular signaling cascades which are normally linked to RANKL.

In order to find suitable treatments for osteolysis, it may be helpful to understand how the molecular mechanisms which support the growth of liposomal CRE-Ter on PLA foams can restrict the process of osteoclastogenesis. Within the canonical NF-κB pathway, RANK ligation could serve to activate IκB kinase complex inhibition, thus creating the phosphorylates NF-κB associated IκBα, and ultimately causing its ubiquitination and

proteasome degradation. As a consequence, NF-κB p65 would be released from the complex, leading to phosphorylation and subsequently its translocation into the nucleus [48]. In the nucleus, NF-κB p65 would bind to the consensus regions of the target genes including TRAP and cathepsin K, thus enhancing their transcription [49]. It has been suggested that the ERK signaling pathway plays an important role in the various processes of osteoclasts, including survival, proliferation, apoptosis, formation, polarity, podosome disassembly, and differentiation. Results obtained from examination of ERK1 knockout and hematopoietic ERK2 conditional knockout mice determined that ERK1 was able to contribute significantly to the modulation of osteoclast differentiation and migration, as well as the resorption of bone [40]. This research has demonstrated that liposomal CRE-Ter which has been grown on PLA foams results in a lowering of NF-κB p65 as well as phosphorylation of NF-κB p65 in line with the size of the dose. CRE-Ter/Liposome grown through PLA foams also decreased expression of the ERK pathway components, ERK and phospho-ERK, in a significant manner ($p < 0.05$). We hypothesised that liposome CRE-Ter acts on the RANK circuit adapter molecules through NF-κB and ERK pathways.

The present study clearly showed that the liposome curcuminoid (CRE-Ter) from turmeric was a new delivery drug system offering anti-osteoclastogenic potential through the restriction, from *in vitro* studies, of RANKL-induced NF-κB and ERK as the main signaling pathways of osteoclastogenesis through the PLA foams. This suggested that the liposomal CRE-Ter delivery drug system might adversely affect the RANKL-induced NF-κB and ERK signaling circuits in line with the concentration applied, and thereby restrict the cathepsin K expression which plays a role in osteoclastogenesis. It would therefore be useful to conduct further research to determine the potential for anti-osteoporotic effects when the liposome CRE-Ter delivery drug system is employed *in vivo*; for instance, by exploring the therapeutic potential in an animal model of osteolysis. Such study would provide further insights on liposome CRE-Ter as an inhibitor of osteoclastogenesis through the PLA foams, thus representing a novel type of drugs for osteolysis.

Declarations

Author contribution statement

Yutthana Pengjam: Conceived and designed the experiments; Performed the experiments; Analyzed and interpreted the data; Contributed reagents, materials, analysis tools or data; Wrote the paper.

Pharkphoom Panichayupakaranant: Contributed reagents, materials, analysis tools or data; Wrote the paper.

Varaporn Tanrattanakul: Contributed reagents, materials, analysis tools or data; Wrote the paper.

Funding statement

This work was supported by the Prince of Songkla University (Grant number MET6202025S) and the Thailand Science Research and Innovation (Grant number MET6405004S).

Data availability statement

No data was used for the research described in the article.

Declaration of interests statement

The authors declare no conflict of interest.

Additional information

No additional information is available for this paper.

References

- [1] K.I. Priyadarsini, The chemistry of curcumin: from extraction to therapeutic agent, *Molecules* 19 (2014) 20091–20112.
- [2] S.K. Sandur, M.K. Pandey, B. Sung, K.S. Ahn, A. Murakami, G. Sethi, P. Limtrakul, V. Badmaev, B.B. Aggarwal, Curcumin, demethoxycurcumin, bisdemethoxycurcumin, tetrahydrocurcumin and turmerones differentially regulate anti-inflammatory and anti-proliferative responses through a ROS-independent mechanism, *Carcinogenesis* 28 (2007) 1765–1773.
- [3] M. Dei Cas, R. Ghidoni, Dietary curcumin: correlation between bioavailability and health potential, *Nutrients* 11 (2019) 2147.
- [4] K.M. Nelson, J.L. Dahlin, J. Bisson, J. Graham, G.F. Pauli, M.A. Walters, The essential medicinal chemistry of curcumin, *J. Med. Chem.* 60 (2017) 1620–1637.
- [5] J.W. Daily, M. Yang, S. Park, Efficacy of turmeric extracts and curcumin for alleviating the symptoms of joint arthritis: a systematic review and meta-analysis of randomized clinical trials, *J. Med. Food* 19 (2016) 717–729.
- [6] S.P. Weisberg, R. Leibel, D.V. Tortoriello, Dietary curcumin significantly improves obesity-associated inflammation and diabetes in mouse models of diabetes, *Endocrinology* 149 (2008) 3549–3558.
- [7] L. Xie, X.-K. Li, S. Takahara, Curcumin has bright prospects for the treatment of multiple sclerosis, *Int. Immunopharm.* 11 (2011) 323–330.
- [8] P. Anand, C. Sundaram, S. Jhurani, A.B. Kunnumakkara, B.B. Aggarwal, Curcumin and cancer: an "old-age" disease with an "age-old" solution, *Canc. Lett.* 267 (2008) 133–164.
- [9] K. Mansouri, S. Rasoulpoor, A. Daneshkhan, S. Abolfathi, N. Salari, M. Mohammadi, S. Rasoulpoor, S. Shabani, Clinical effects of curcumin in enhancing cancer therapy: a systematic review, *BMC Canc.* 20 (2020) 791.
- [10] G. Antonio, G. Tommonaro, Curcumin and cancer, *Nutrients* 11 (2019) 2376.
- [11] K. Ikeda, S. Takeshita, The role of osteoclast differentiation and function in skeletal homeostasis, *J. Biochem.* 159 (2016) 1–8.
- [12] W.J. Boyle, W.S. Simonet, D.L. Lacey, Osteoclast differentiation and activation, *Nature* 423 (2003) 337–342.
- [13] B.F. Boyce, Y. Xiu, J. Li, L. Xing, Z. Yao, NF- κ B-Mediated regulation of osteoclastogenesis, *Endocrinol. Metabol.* (Seoul, Korea) 30 (2015) 35–44.
- [14] M. Nakamura, N. Aoyama, S. Yamaguchi, Y. Sasano, Expression of tartrate-resistant acid phosphatase and cathepsin K during osteoclast differentiation in developing mouse mandibles, *Biomed. Res.* 42 (2021) 13–21.
- [15] P. Du Souich, Absorption, distribution and mechanism of action of SYSADOAS, *Pharmacol. Ther.* 142 (2014) 362–374.
- [16] Y. Pengjam, H. Madhyastha, R. Madhyastha, Y. Yamaguchi, Y. Nakajima, M. Maruyama, NF- κ B pathway inhibition by anthrocylic glycoside aloin is key event in preventing osteoclastogenesis in RAW264.7 cells, *Phytomedicine* 23 (2016) 417–428.
- [17] A.C. Bharti, Y. Takada, B.B. Aggarwal, Curcumin (diferuloylmethane) inhibits receptor activator of NF- κ B ligand-induced NF- κ B activation in osteoclast precursors and suppresses osteoclastogenesis, *J. Immunol.* 172 (2004) 5940–5947.
- [18] B. Dhanyayuthapani, Y. Yoshida, T. Maekawa, D. Kumar, Polymeric scaffolds in tissue engineering application: a review, *Int. J. Polym. Sci.* 290602 (2011) 1–19.
- [19] M. Vallet-Regí, E. Ruiz-Hernández, Bioceramics: from bone regeneration to cancer nanomedicine, *Adv. Mater.* 23 (2011) 5177–5218.
- [20] S. Bose, S. Vahabzadeh, A. Bandyopadhyay, Bone tissue engineering using 3D printing, *Mater. Today* 16 (2013) 496–504.
- [21] P. Sungsee, V. Tanrattanakul, Biocomposite foams from poly(lactic acid) and rubber wood sawdust: mechanical properties, cytotoxicity, and in vitro degradation, *J. Appl. Polym. Sci.* 136 (2019) 48259.
- [22] P. Anand, A.B. Kunnumakkara, R.A. Newman, B.B. Aggarwal, Bioavailability of curcumin: problems and promises, *Mol. Pharm.* 4 (2007) 807–818.
- [23] S.S. Bansal, M. Goel, F. Aqil, M.V. Vadhanam, R.C. Gupta, Advanced drug delivery systems of curcumin for cancer chemo prevention, *Canc. Prev. Res.* 4 (2011) 1158–1171.
- [24] L. Lateh, L.; Kaewnopparat, N.; Panichayupakaranant, P., A method for increasing the water-solubility of curcuminoids and its products. Petty Patent 2018, No. 14639, Thailand.
- [25] L. Lateh, S. Yuenyongsawad, H. Chen, P. Panichayupakaranant, A green method for preparation of curcuminoid-rich *Curcuma longa* extract and evaluation of its anticancer activity, *Phcog. Mag.* 15 (2019) 730–735.
- [26] R. Pochampally, V. John, A. Alb, J. He, G. Tan, J. Feldman, R. Walker, T. Frazier, P. Penforis, S.S. Dhule, Curcumin-loaded γ -cyclodextrin liposomal nanoparticles as delivery vehicles for osteosarcoma, *Nanomed. Cancer: Pan Stanford* (2017) 291–322.
- [27] L. Sercombe, T. Veerati, F. Moheimani, S.Y. Wu, A.K. Sood, S. Hua, Advances and challenges of liposome assisted drug delivery, *Front. Pharmacol.* 6 (2015) 286.
- [28] T. Feng, Y. Wei, R. Lee, L. Zhao, Liposomal curcumin and its application in cancer, *Int. J. Nanomed.* 12 (2017) 6027.
- [29] A. Akbarzadeh, R. Rezaei-Sadabady, S. Davaran, S.W. Joo, N. Zarghami, Y. Hanifehpour, M. Samiei, M. Kouhi, K. Nejati-Koshki, Liposome: classification, preparation, and applications, *Nanoscale Res. Lett.* 8 (2013) 102.
- [30] N. Sarkar, S. Bose, Liposome-encapsulated curcumin-loaded 3D printed scaffold for bone tissue engineering, *ACS Appl. Mater. Interfaces* 11 (2019) 17184–17192.
- [31] M. Viale, A. Fontana, I. Maric, M. Monticone, G. Angelini, C. Gasbarri, Preparation and antiproliferative activity of liposomes containing a combination of cisplatin and procainamide hydrochloride, *Chem. Res. Toxicol.* 29 (2016) 1393–1395.
- [32] S. Mammana, A. Gugliandolo, E. Cavalli, F. Diomedede, R. Iori, R. Zappacosta, P. Bramanti, P. Conti, A. Fontana, J. Pizzicannella, E. Mazzon, Human gingival mesenchymal stem cells (GMSCs) pretreated with vesicular moringin nanostructures as a new therapeutic approach in a mouse model of spinal cord injury, *J. Tissue Eng. Regen. Med.* 13 (2019) 1109–1121.
- [34] B. Sinjari, J. Pizzicannella, M. D'Aurora, R. Zappacosta, V. Gatta, A. Fontana, O. Trubiani, F. Diomedede, Curcumin/liposome nanotechnology as delivery platform for anti-inflammatory activity via NF κ B/ERK/pERK pathway in human dental pulp treated with 2-hydroxyethyl methacrylate (HEMA), *Front. Physiol.* 10 (2019) 1–11.
- [35] B. Basnet, H. Hussain, I. Tho, N. Skalko-Basnet, Liposomal delivery system enhances anti-inflammatory properties of curcumin, *J. Pharm. Sci.* 101 (2012) 598–609.
- [36] D.Y. Zuo, Y. Wang, W.L. Xu, H.T. Liu, Effects of polyvinylpyrrolidone on structure and performance of composite scaffold of chitosan superfine powder and polyurethane, *Adv. Polym. Technol.* 3 (2012) 310–318.
- [37] P. Basu, N. Saha, R. Alexandrova, P. Saha, Calcium phosphate incorporated bacterial cellulose-polyvinylpyrrolidone based hydrogel scaffold: structural property and cell viability study for bone regeneration application, *Polymers* 11 (2019) 1821.
- [38] A.M. Fernández-Romero, F. Maestrelli, P.A. Mura, A.M. Rabasco, M.L. González-Rodríguez, Novel findings about double-loaded curcumin-in-HP β Cyclodextrin-in liposomes: effects on the lipid bilayer and drug release, *Pharmaceutics* 10 (2018) 256.
- [39] J.H. Kim, E.Y. Kim, B. Lee, J.H. Min, D.U. Song, J.M. Lim, The effects of Lycii Radix Cortex on RANKL-induced osteoclast differentiation and activation in RAW 264.7 cells, *Int. J. Mol. Sci.* 37 (2016) 649–658.
- [40] K. Lee, I. Seo, M.H. Choi, D. Jeong, Roles of mitogen-activated protein kinases in osteoclast biology, *Int. J. Mol. Sci.* 19 (2018) 3004.
- [41] J. Morko, R. Kiviranta, M.T. Mulari, K.K. Ivaska, H.K. Väänänen, E. Vuorio, T. Laitala-Leinonen, Overexpression of cathepsin K accelerates the resorption cycle and osteoblast differentiation in vitro, *Bone* 44 (2009) 717–728.
- [42] R. Chang, L. Sun, T.J. Webster, Short communication: selective cytotoxicity of curcumin on osteosarcoma cells compared to healthy osteoblasts, *Int. J. Nanomed.* 9 (2014) 461.
- [43] C. Yang, K. Zhu, X. Yuan, X. Zhang, Y. Qian, T. Cheng, Curcumin has immunomodulatory effects on RANKL-stimulated osteoclastogenesis in vitro and titanium nanoparticle-induced bone loss in vivo, *J. Cell Mol. Med.* 24 (2020) 1553–1567.
- [44] C.C. Yeh, Y.H. Su, Y.J. Lin, P.J. Chen, C.S. Shi, C.N. Chen, H.I. Chang, Evaluation of the protective effects of curcuminoid (curcumin and bisdemethoxycurcumin)-loaded liposomes against bone turnover in a cell-based model of osteoarthritis, *Drug Des. Dev. Ther.* 9 (2015) 2285–2300.
- [45] C. Cheng, S.F. Peng, Z.L. Li, L.Q. Zou, W. Liu, C.M. Liu, Improved bioavailability of curcumin in liposomes prepared using a pH-driven, organic solvent-free, easily scalable process, *RSC Adv.* 7 (2017) 25978–25986.
- [46] M.S. Lopes, A.L. Jardini, M. Filhom, Poly (lactic acid) production for tissue engineering applications, *Procedia Eng.* 42 (2012) 1402–1413.
- [47] B.Y. Chen, X. Jing, H.Y. Mi, H. Zhao, W.H. Zhang, X.F. Peng, L.S. Turng, Fabrication of poly(lactic acid)/poly(ethylene glycol) (PLA/PEG) porous scaffold by supercritical CO₂ foaming and particle leaching, *Polym. Eng. Sci.* 55 (2015) 1339.
- [48] Y. Abu-Amer, NF- κ B signaling and bone resorption, *Osteoporos. Int.* 24 (2013) 2377–2386.
- [49] B.H. Kim, J.H. Oh, N.K. Lee, The inactivation of ERK1/2, p38 and NF- κ B is involved in the down-regulation of osteoclastogenesis and function by A2B adenosine receptor stimulation, *Mol. Cell.* 40 (2017) 752–760.